Mechanically tunable dual-band metamaterial absorber at ultra-high frequency

Duong Thi Ha[1, 3], Vankham Boudthaly[3], Soulima Khamsadeth[3], Vu Thi Hong Hanh[3], Bui Son Tung[1, 2**], Bui Xuan Khuyen[1, 2**], Vu Dinh Lam[1*]

[1]Graduate University of Science and Technology, Vietnam Academy of Science and Technology;
[2]Institute of Materials Science, Vietnam Academy of Science and Technology;
[3]Thai Nguyen University of Education, Thai Nguyen University.
[*]Corresponding author: lamvd@gust-edu.vast.vn
[**]Co-Corresponding authors: khuyenbx@ims.vast.ac.vn; tungbs@ims.vast.ac.vn
Received 13 Oct 2022; Revised 15 Nov 2022; Accepted 12 Dec 2022; Published 28 Dec 2022.
DOI: https://doi.org/10.54939/1859-1043.j.mst.84.2022.93-100

ABSTRACT

We numerically demonstrated a dual-band metamaterial absorber (MPA) operating in low frequency range based on a flexible polyimide substrate. For the flat configuration, two absorption peaks are obtained at 450 MHz and 1.47 GHz with absorption over 90%. The ratios of the periodicity of unit cells and thickness to the longest absorption wavelength are 1/12 and 1/114, respectively. Especially, our MPA is insensitive with polarization and stable with the oblique incidence angle of incoming electromagnetic waves. The proposed MPA maintains an absorption over 90% when incident angle is increased up to 60^o. Furthermore, since structure is wrapped and attached to cylindered surfaces (the varying radii from 200 to 500 mm), new absorption peaks can be obtained at higher frequency range. For both flat and curvature states, the absorption mechanism is explained by the magnetic resonance and the perfect impedance matching phenomena.

Keywords: Mechanically tunable; Dual-band; Metamaterial absorber; Ultra-high frequency.

1. INTRODUCTION

Metamaterials (MMs) are well-known as man-made structures which possess novel properties not found in natural materials. After being experimentally proven by Smith *et al.* in 2000 [1], MMs has attached much of attention and discovered interesting new effects and technologies such as negative refractive indices [1], perfect lenses [2], backward Cherenkov radiation [3], inverse Doppler effect [4] etc. In particular, a fascinating ability that MMs can achieve unity absorption was the first introduced by Landy *et al.* in 2008 and these MMs were called metamaterial perfect absorber (MPA) [5]. The great advancement of MPAs that are thin thickness and high-performance efficiency, so MPA has been become an outstanding candidate for a wide-range application areas, such as sensors [6, 7], energy harvesting [8, 9], images [10,11], radar target stealth [12], etc. operating in various frequency ranges from the microwave [6, 13-15] to optical range [16, 17].

In recent years, telecommunication technology has developed rapidly, the potential application of MPA has been extended to many devices operating in lower frequency region such as power imaging purposes [18], chipless radio-frequency identification tags [19], and sub-GHz wireless systems [20]. However, the designing MPA for reality applications at low frequencies is challenging. Firstly, MPA is required to have high-efficiency absorption in low frequency bands with compact structure and light weight. To overcome this challenge, various efficient methods have been developed. One of popular approaches is that integrating the lumped elements into the designed structure. For example, Khuyen *et al.* exploited the lumped capacitors with through interconnects, the unit-cell size of their MPA was miniaturized to be λ/816 at 102 MHz [21]. In 2018, Li *et al.* obtained a thin and ultra-broadband MPA with absorption over 80% for the range

of 20.98 GHz (from 4.48 to 25.46 GHz) by using multi-layered resonators lumped with 4 resistors [22]. Beside using lumped elements, optimizing the structure was also utilized to achieve miniaturization for MPA in low frequency band. Remarkably, Yoo *et al.* designed a snake-shaped MPA to scale down the size of unit cell to be λ/30 and λ/40 for the resonant frequency of 400 MHz [23]. In the ultra-high frequency (UHF) band, Fan *et. al*. obtained an MPA with small-size unit cell by combining fractal and coupling lines [24]. Their absorber induced an absorption peak at 442 MHz while the ratio between size of unit cell and absorption wavelength is only 1/68. So far, the inflexibility can be regarded as the second challenge for practical applications of recent MPAs in UHF band (300 MHz - 3 GHz). In general, MPA is constructed with a three layered structure, in which the dielectric layer is hard, so it is limited in practical applications, especially in the case of wrapping the rough surfaces. This problem can be solved by replacing rigid dielectric layer by flexible substrates such as paper, polyimide, ultralam substrates. Recently, there are several works in which flexible substrates have been exploited for MPA [23-25], however the influence of curvature states on the absorption properties of MPA structure have been not yet surveyed sufficiently.

In this work, we introduce a dual-band MPA using a good flexibility substrate (polyimide). By a proper design, a dual-band absorption at UHF band was induced by the fundamental and third-order magnetic resonance. For these both peaks, the dependence of absorption spectra on the incident angle and polarization angle of electromagnetic (EM) waves wave was investigated in detail. Moreover, the simulated results for curvature configuration reveal that, there are new peaks appear at the higher frequency range.

2. STRUCTURE DESIGN AND METHODS

The unit cell of the proposed MPA is depicted in Fig. 1. Its structure includes three layers: a periodic folded-line structure on the top, a dielectric spacer at the middle and a continuous metal plate at the bottom. The top and bottom layers are made of copper with a thickness of t_m = 0.035 mm and the electric conductivity of 5.96 x 10^7 S/m. To achieve the flexible property, a polyimide substrate with a dielectric constant of 3.5 and a loss tangent of 0.0027 is chosen as the dielectric layer. Such a three-layer material configuration has been successfully fabricated in which the metal layers adhere very well to the polyimide dielectric layer, and they are stable in curvature state with different bending radii [26]. The key geometrical parameters of designed structure are the size of unit cell, the thickness of dielectric layer, the width and length of folding lines and the gap between them. In order to obtained the best absorption performance, the values of these parameters are optimized and illustrated in table 1.

Table 1. *Optimized geometrical parameters of MPA.*

Geometrical parameters	*a*	*p*	*t*	w_1	w_2	w_3	l_1	l_2	l_3	l_4
Value (mm)	55	54.5	4	2.8	0.6	0.5	7.2	6.5	13.5	20

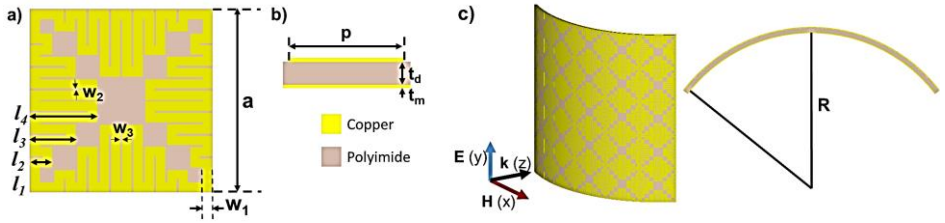

Figure 1. *Schematic of the unit cell: (a) Top view; (b) Side view; (c) Bending model with radius R.*

Our simulation is carried out by using the commercial Computer Simulation Technology (CST) Microwave Studio [27]. In this simulation, the boundary conditions are set to be the unit cells for x- and y-directions and open for the z direction. The absorption is calculated by $A(\omega) = 1 - R(\omega) -$

$T(\omega)$, where $R(\omega) = |S_{11}|^2$ and $T(\omega) = |S_{21}|^2$ are the reflection and the transmission coefficient, respectively. Due to the appearance of continuous metallic plane at the bottom, the transmission is vanished, and then the absorption can be simplified as: $A(\omega) = 1 - R(\omega)$.

3. RESULTS AND DISCUSSION

Firstly, we simulate the absorption of the proposed MPA for normal incidence of EM wave in the planar configuration. The simulated results are presented in Fig. 2. It is clear that, two nearly-perfect absorption peaks are obtained at 450 MHz and 1.47 GHz with absorptions of 99.4% and 99.8%, respectively. It is noteworthy that the thickness of MPA is miniaturized to be only $\lambda/114$, in which λ is the longest absorption wavelength (in mm). This value is smaller than those of previous works [24, 28-30]. The mechanism of perfect absorption can be explicated using the impedance-matching theory, where the effective impedance of the proposed MPA can be calculated based on the extracted S-parameters as following expression [31]:

$$Z(\omega) = \sqrt{\frac{\left(1 + S_{11}(\omega)\right)^2 - S_{21}^2(\omega)}{\left(1 - S_{11}(\omega)\right)^2 - S_{21}^2(\omega)}} \quad (1)$$

Fig. 2(b) shows the real and the imaginary parts of the effective impedance in the MHz range. Obviously, the real part is about 1.08 and the imaginary part is zero at 450 MHz, which reveals that the effective impedance is nearly equal to the free space impedance. We also calculate the effective impedance of MPA in the GHz range as plotted in Fig. 2(d). Similarly, at the absorption frequency of 1.47 GHz, the values of imaginary and real parts of the effective impedance are zero and approximate 1.0, respectively. These values confirm that the effective impedance of MPA is matched well with free space. Consequently, at 450 MHz and 1.47 GHz, there is no reflection wave and the incoming wave can be captured inside the MPA.

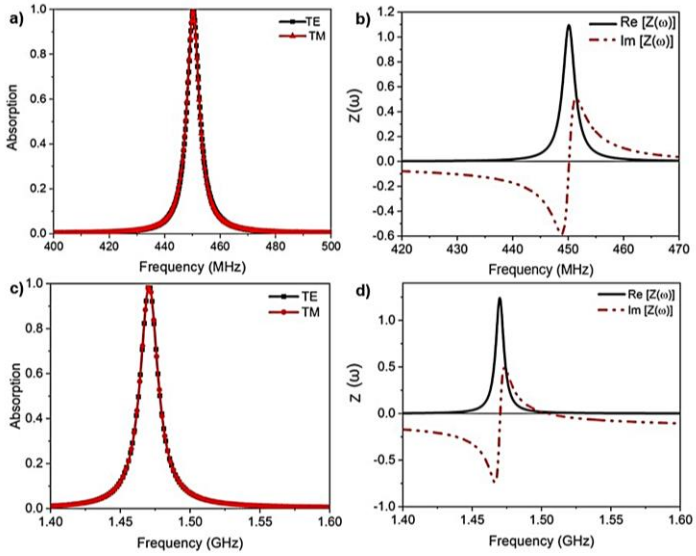

Figure 2. *(a) Absorption spectrum and (b) effective impedance of the MPA in MHz range, (c) Absorption spectrum and (d) effective impedance of the MPA in GHz range.*

To investigate the physical mechanism of perfect absorption, the distributions of induced surface current on the meta-surfaces are simulated at 450 MHz and 1.47 GHz, as shown in Fig. 3. At 450 MHz, the top- and bottom-induced surface currents are opposite directions, as presented in Fig. 3(a), which confirm that the absorption mechanism is ruled by the fundamental magnetic resonance [32]. Meanwhile, at higher absorption peak (1.47 GHz), the induced surface currents

are divided into three separated regions and these currents in each region are anti-parallel, as indicated in Fig. 3(b). Therefore, there are three current loops, which are all created between the top and bottom copper layers. These phenomena confirm that, the second perfect absorption (at 1.47 GHz) is originated from the third-order magnetic resonance [33].

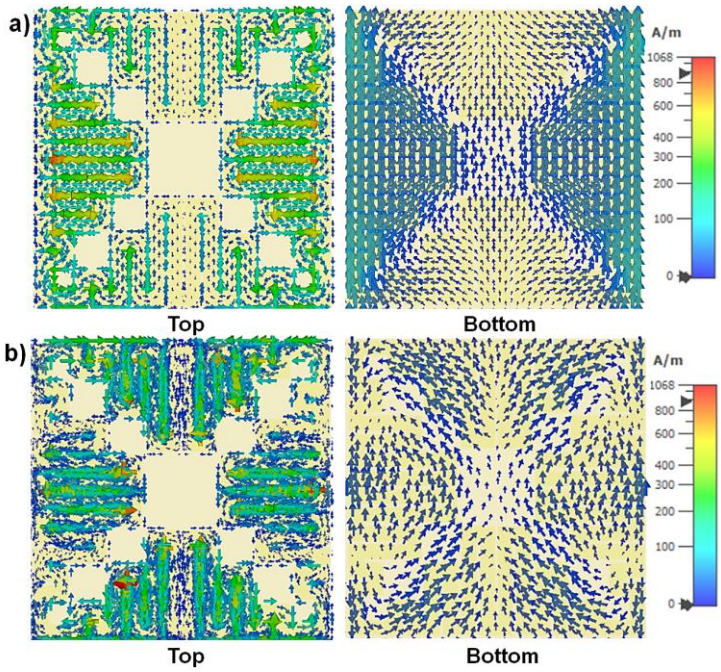

Figure 3. *Distributions of induced-surface-currents on the metallic layers of MPA at (a) 450 MHz and (b) 1.47 GHz.*

The influence of incidence angle of EM wave on absorption feature of flat MPA is investigated and illustrated in Fig. 4. For the case of absorption peak at 450 MHz, since the incident angle is increased from 0^o to 60^o, the absorptions maintain above 90% and slightly shifts to the higher frequency for both TE and TM polarization wave, as shown in Figs. 4(a) and 4(b), reflectively. As the incident angle is increased up to 75^o, the absorption falls to below 65% for the TE polarization and to 83% for the TM case. At 1.47 GHz, for both TE and TM polarizations, the absorption is still remained to be over 90%, when the incident angle is increased from 0^o to 60^o. However, at larger incident angles, the absorption peak is shifted to lower frequency range (for the case of TE polarization), whereas it is shifted towards high frequencies (for the case of TM polarization). Besides, our MPA is designed with high symmetry, so it is polarization-insensitive, as has been shown in previous works [25, 34].

It can be noted that, one advantage of using flexible substrate over stiff dielectric material is that we can simply wrap or attach MPA on a rough surface (for example cylindrical surface). Secondary, for practical uses, the proposed absorber should be mechanically flexible to be able to bend with bending radii in the range from 100 mm to 500 mm. In this simulation, a full structure of MPA is constructed and simulated for the TE polarization of the EM wave. The plan wave propagates along the z-direction while the electric field and magnetic field are set to be along the y- and x-directions, respectively. Firstly, the influence of curvature on absorption performance of MPA structure in the MHz frequency range is studied and shown in Fig. 5(a). As the bending radius of 500 mm, there is a new absorption peak raised at 556 MHz with the absorption of 73% while the absorption of original absorption peak at 450 MHz falls to below 28%. The absorption of initial peak reduces to only about 10% when the bending radius is decreased to be 200mm, whereas the absorption at 556 MHz is reached to be nearly 90%.

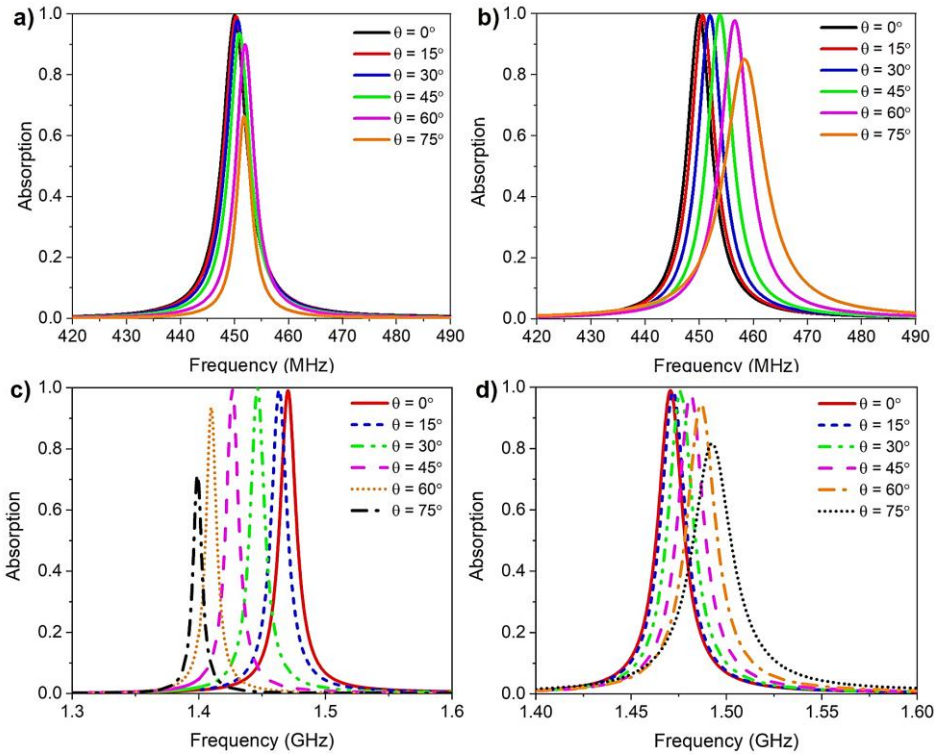

Figure 4. *Dependence of absorption spectra on different oblique incident angles with (a)-(c) TE polarization and (b)-(d) TM polarization, in MHz and GHz regions.*

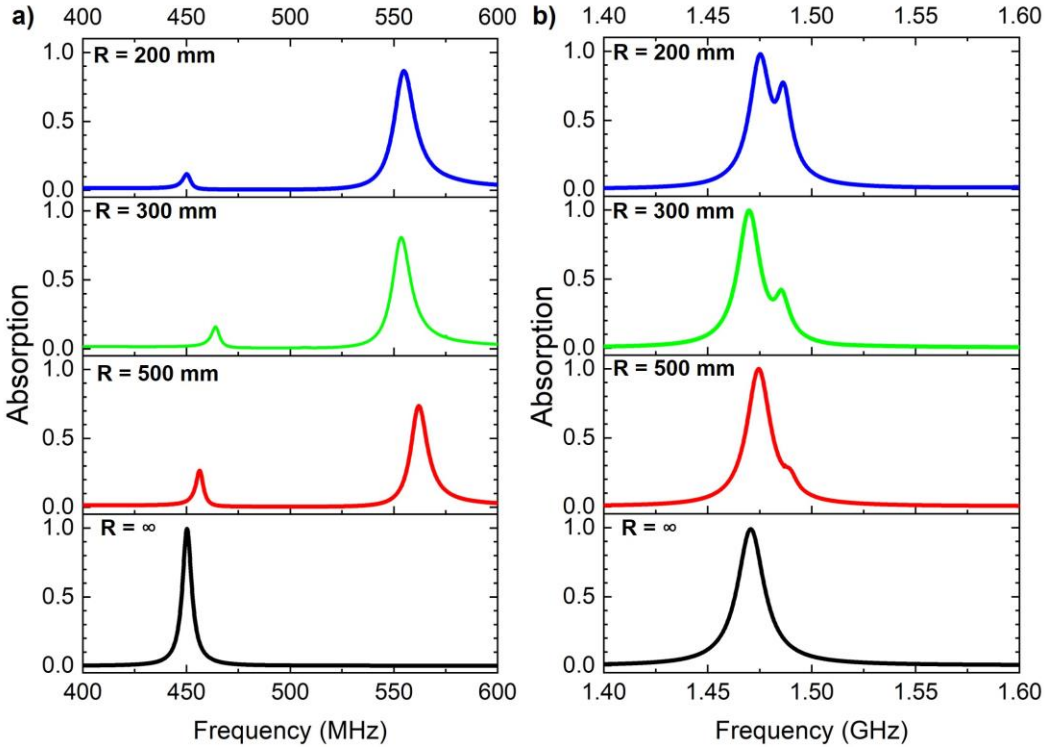

Figure 5. *Dependence of the simulated absorption spectrum on bending radius for (a) fundamental absorption peak and (b) high-order one.*

For the GHz range, the impact of curvature to the absorption characteristics of MPA structure is also considered and shown in Fig. 5(b). When the MPA is bent, the initial high-order absorption peak at 1.47 GHz is divided into two absorption peaks, where a new absorption peak is formed at higher frequency (1.48 GHz). The bending radius is tuned to be decrease, the absorption at 1.48 GHz is increased to be nearly 79%, while the absorption of initial high-order peak is still remained. The appearance of new high-order absorption peaks can be explained by the asymmetric structure at different bending states.

The distribution of induced surface current for the case of the radius bending R = 200 mm is presented in Fig. 6. At 450 MHz and 1.47 GHz, strong surface currents are induced at the position of unit cells around the center of the semi-cylinder. Whereas, at 556 MHz and 1.48 GHz, strong surface currents are induced at the position of the unit cells on the edges of the semi-cylinder. This phenomenon indicates that, differently from the dependence of oblique incidence, the bending state of the MPA structure makes the distribution of electric- and magnetic-fields on the MPA surface to be inhomogeneous, which induces new resonance absorption peaks [35, 36]. The observed of new peak in bending configuration is similar to previous works, which have shown that, additional absorption peaks appeared due to the severe asymmetry of bent structure [26].

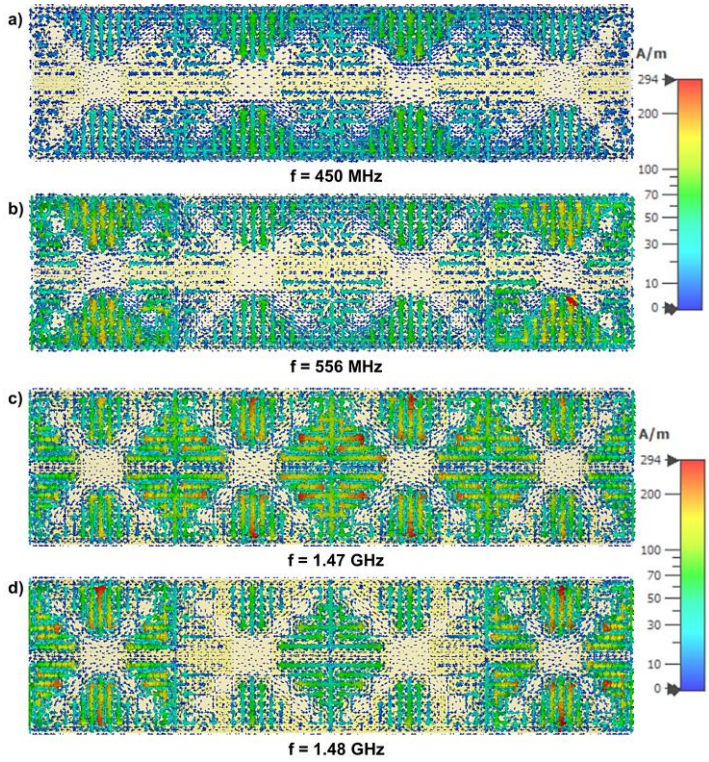

Figure 6. *Surface-current distribution on the metallic layers of MPA with bending radius R = 200 mm, for the case of TE polarization at different frequencies.*

4. CONCLUSIONS

In this work, a dual-band flexible MPA operating in the UHF band is investigated numerically. The MPA structure consisted of a periodic array of a folding line to obtain two resonant peaks at 450 MHz and 1.47 GHz. The ratios of the periodicity of unit cells and thickness to the fundamental absorption wavelength are 1/12 and 1/114, respectively. The MPA shows absorptivity above 90% at 450 MHz and 1.47 GHz remained relatively stable under wide range of incident angles from 0^o to 60^o for both TE and TM polarizations. The new two absorption peaks are

tuned when MPA is bent with different bending radius. The physical mechanism of the MPA structure is clarified from magnetic-resonance and impedance-matching phenomena. These achieved results could be useful for future marketable applications of flexible, polarization/oblique-incidence insensitive, low-cost and ultrathin-wearable modern electronic devices.

Acknowledgement: *This research was funded by the Vietnam National Foundation for Science and Technology Development (NAFOSTED) under grant number 103.99–2020.23. Duong Thi Ha was funded by Vingroup JSC and supported by the Master, PhD Scholarship Programme of Vingroup Innovation Foundation (VINIF), Institute of Big Data, code VINIF.2021.TS.092.*

REFERENCES

[1]. D. R. Smith, W. J. Padilla, D. Vier, S. C. Nemat-Nasser, S. Schultz, *"Composite medium with simultaneously negative permeability and permittivity"*, Phys. Rev. Lett., 84, 4184, (2000).

[2]. Y. J. Yoo, C. Yi, J. S. Hwang, Y. J. Kim, S. Y. Park, K. W. Kim, J. Y. Rhee, Y. Lee, *"Experimental realization of tunable metamaterial hyper-transmitter"*, Sci. Rep., 6(1), pp. 1 - 8, (2016).

[3]. Z. Duan, X. Tang, Z. Wang, Y. Zhang, X. Chen, M. Chen, Y. Gong, *"Observation of the reversed Cherenkov radiation"*, Nat. Commun., 8, 14901, (2017).

[4]. N. Seddon, T. Bearpark, *"Observation of the inverse Doppler effect"*, Science, 302, 1537, (2003).

[5]. N. I. Landy, S. Sajuyigbe, J. J. Mock, D. R. Smith, W. J. Padilla, *"Perfect metamaterial absorber"*, Phys. Rev. Lett., 100, 207402, (2008).

[6]. M. Bakır, M. Karaaslan, E. Unal, O. Akgol, C. Sabah, *"Microwave metamaterial absorber for sensing applications"*, Opto-Electron. Rev., 25(4), pp. 318 - 325, (2017)

[7]. A. Mohanty, O. P. Acharya, B. Appasani, S. K. Mohapatra, M. S. Khan, *"Design of a novel terahertz metamaterial absorber for sensing applications"*, IEEE Sen. J., 21(20), pp. 22688 - 22694, (2021).

[8]. G. E. Persis, J. J. Paul, T. B. Mary, R. C. Joy, *"A compact tilted split ring multiband metamaterial absorber for energy harvesting applications"*, Mater. Today: Proc., 56, pp. 368 - 372, (2022).

[9]. A. Elsharabasy, M. Bakr, M. J. Deen, *"Wide-angle, wide-band, polarization-insensitive metamaterial absorber for thermal energy harvesting"*, Sci. Rep., 10(1), pp. 1 - 10, (2020.)

[10]. D. Hu, T. Meng, H. Wang, Y. Ma, Q. Zhu, *"Ultra-narrow-band terahertz perfect metamaterial absorber for refractive index sensing application"*, Results Phys., 19, p.103567, (2020).

[11]. C. Gong, M. Zhan, J. Yang, Z. Wang, H. Liu, Y. Zhao, W. Liu, *"Broadband terahertz metamaterial absorber based on sectional asymmetric structures"*, Sci. Rep., 6(1), pp. 1 - 8, (2016).

[12]. M. Li, Z. Yi, Y. Luo, B. Muneer, Q. Zhu, *"A novel integrated switchable absorber and radiator"*, IEEE Trans. Antennas Propag., 64, no. 3, pp. 944 - 952, (2016).

[13]. M. C. Tran, V. H. Pham, T. H. Ho, T. T. Nguyen, H. T. Do, X. K. Bui, S. T. Bui, D. T. Le, T. L. Pham, D. L. Vu, *"Broadband microwave coding metamaterial absorbers"*, Sci. Rep., 10(1), pp. 1 - 11 (2020).

[14]. Z. Zhang, L. Zhang, X. Chen, Z. Wu, Y. He, Y. Lv, Y. Zou, *"Broadband metamaterial absorber for low-frequency microwave absorption in the S-band and C-band"*, J. Magn. Magn. Mater., 497, p. 166075, (2020).

[15]. M. R. Soheilifar, *"Design, fabrication, and characterization of scaled and stacked layers metamaterial absorber in microwave region"*, Microw. Opt. Technol. Lett., 58(5), pp. 1187 - 1193, (2016).

[16]. P. Yu, L. V. Besteiro, J. Wu, Y. Huang, Y. Wang, A. O. Govorov, Z. Wang, *"Metamaterial perfect absorber with unabated size-independent absorption"*, Opt. Express, 26(16), pp. 20471 - 20480, (2018).

[17]. A. Musa, M. L. Hakim, T. Alam, M. T. Islam, A. S. Alshammari, K. Mat, S. H. Almalki, M. S. Islam, *"Polarization Independent Metamaterial Absorber with Anti-Reflection Coating Nanoarchitectonics for Visible and Infrared Window Applications"*, Materials, 15(10), p. 3733, (2022).

[18]. S. Yagitani, K. Katsuda, M. Nojima, Y. Yoshimura, H. Sugiura, *"Imaging radio-frequency power distributions by an EBG absorber"*, IEICE Trans. Commun. E, 94-B, 2306, (2011).

[19]. F. Costa, S. Genovesi, A. Monorchio, *"A chipless RFID based on multiresonant high-impedance surfaces"*, IEEE Trans. Microwave Theory Tech., 61, 146, (2013).

[20]. F. Costa, S. Genovesi, A. Monorchio, G. Manara, *"On the bandwidth of high-impedance frequency selective surfaces"*, IEEE Antennas Wireless Propag. Lett., 8, 1341, (2009).

[21]. B.X. Khuyen, B.S. Tung, Y.J. Yoo, Y.J. Kim, K.W. Kim, L.-Y. Chen, V.D. Lam, Y.P. Lee, *"Miniaturization for ultrathin metamaterial perfect absorber in the VHF band"*, Sci. Rep., 7, 45151, (2017).

[22]. S. J. Li, P. X. Wu, H. X. Xu, Y. L. Zhou, X. Y. Cao, J. F. Han, C. Zhang, H. H. Yang, Z. Zhang, *"Ultra-wideband and polarization-insensitive perfect absorber using multilayer metamaterials, lumped resistors, and strong coupling effects"*, Nano Res. Lett., 13(1), 386, (2018).

[23]. Y. J. Yoo, H. Y. Zheng, Y. J. Kim, J. Y. Rhee, J. H. Kang, K. W. Kim, H. Cheong, Y. H. Kim, Y. P. Lee, *"Flexible and elastic metamaterial absorber for low frequency, based on small size unit cell"*, Appl. Phys. Lett., 105**,** 041902, (2014).

[24]. S. Fan, Y. Song, *"UHF metamaterial absorber with small-size unit cell by combining fractal and coupling lines"*, Int. J. Antennas Propag., (2018).

[25]. B. X. Khuyen, B. S. Tung, Y. J. Kim, J. S. Hwang, K. W. Kim, J. Y. Rhee, V. D. Lam, Y. H. Kim, Y. Lee, *"Ultra-subwavelength thickness for dual/triple-band metamaterial absorber at very low frequency"*, Sci. Rep., 8(1), 11632, (2018).

[26]. D. T. Ha, B. S. Tung, B. X. Khuyen, T. S. Pham, N. T. Tung, N. H. Tung, N. T. Hoa, V. D. Lam, H. Zheng, L. Chen, Y. Lee, "*Dual-Band, Polarization-Insensitive, Ultrathin and Flexible Metamaterial Absorber Based on High-Order Magnetic Resonance*", Photonics, 8(21), p. 574, (2021).

[27]. CST Microwave Studio 2015, License ID: 52856-1. Dassault Systèmes. Available online: http://www.cst.com (accessed on 15 June 2021).

[28]. B. X. Khuyen, B. S. Tung, N. V. Dung, Y. J. Yoo, Y. J. Kim, K. W. Kim, V. D. Lam, J. G. Yang, Y. Lee, *"Size-efficient metamaterial absorber at low frequencies: Design, fabrication, and characterization"*, J. Appl. Phys., 117(24), p. 243105, (2015).

[29]. Y. J. Yoo, H. Y. Zheng, Y. J. Kim, J. Y. Rhee, J. H. Kang, K. W. Kim, H. Cheong, Y. H. Kim, Y. P Lee, "*Flexible and elastic metamaterial absorber for low frequency, based on small-size unit cell*", Appl. Phys. Lett., 105 (4), 041902, (2014).

[30]. B. Lin, S. Zhao, X. Da, Y. Fang, J. Ma, W. Li, Z. Zhu, "*Triple-band low frequency ultracompact metamaterial absorber*", J. Appl. Phys., 117(18), 184503, (2015).

[31]. X. Chen, T. M. Grzegorczyk, B. I. Wu, J. Pacheco Jr, J. A. Kong, *"Robust method to retrieve the constitutive effective parameters of metamaterials"*, Phys. Rev. E, *70*, 016608 (2004).

[32]. J. Zhou, E. N. Economon, T. Koschny, C. M. Soukoulis, *"Unifying approach to left-handed material design"*, Opt. Lett., *31*, 3620 - 3622, (2006**).**

[33]. S. Jung, Y. J. Kim, Y. J. Yoo, J. S. Hwang, B. X. Khuyen, L. Y. Chen, Y. Lee, *"High-order resonance in a multiband metamaterial absorber"*, J. Electron. Mater., 49(3), pp.1677 - 1688, (2020).

[34]. M. L. Hakim, T. Alam, A. F. Almutairi, M. F. Mansor, M. T. Islam, "*Polarization insensitivity characterization of dual-band perfect metamaterial absorber for K band sensing applications*", Sci. Rep., 11(1), pp. 1 - 14, (2021).

[35]. J. S. Hwang, Y. J. Kim, Y. J. Yoo, K. W. Kim, J. Y. Rhee, L. Y. Chen, Y. P. Lee, *"Switching and extension of transmission response, based on bending metamaterials"*, Sci. Rep., 7, pp. 3559, (2017).

[36]. V. Aksyuk, B. Lahiri, G. Holland, A. Centrone, *"Near-field asymmetries in plasmonic resonators"*, Nanoscale, 7, pp. 3634 - 3644 (2015).

TÓM TẮT

Điều khiển vật liệu biến hóa hấp thụ sóng điện từ dải kép trong vùng tần số UHF bằng tác động cơ học

Chúng tôi nghiên cứu mô phỏng một cấu trúc vật liệu biến hóa hấp thụ sóng tuyệt đối sóng điện từ (MPA) băng tần kép hoạt động trong vùng tần số thấp, dựa trên đế polyimide có đặc tính đàn hồi. Khi vật liệu ở dạng phẳng, hai cực đại hấp thụ thu được tại tần số 450 MHz và 1,47 GHz với độ hấp thụ đạt trên 90%. Kích thước của ô cơ sở và độ dày của MPA tương ứng bằng 1/12 và 1/114 bước sóng tại tần số hấp thụ thấp nhất. Đặc biệt, MPA được đề xuất không nhạy với góc phân cực và hoạt động ổn định dưới góc tới rộng của sóng điện từ (duy trì độ hấp thụ cao hơn 90% khi góc tới lên đến 60^o). Bên cạnh đó, khi cấu trúc được uốn cong (bán kính uốn cong khác nhau thay đổi từ 200 đến 500 mm) bằng tác động cơ học, các đỉnh hấp thụ mới được hình thành do sự bất đối xứng của cấu trúc. Đối với cả trạng thái phẳng và uốn cong, cơ chế hấp thụ được giải thích thông qua hiệu ứng cộng hưởng từ và sự phối hợp trở kháng hoàn hảo.

Từ khoá: Điều khiển cơ học; Hấp thụ dải kép; Vật liệu biến hóa hấp thụ sóng điện từ; Vùng tần số UHF.